Ultrashort 1-kHz laser plasma hard x-ray source

Georg Korn, Andreas Thoss, Holger Stiel, Ullrich Vogt, Martin Richardson,* and Thomas Elsaesser

Max-Born-Institut für Nichtlineare Optik und Kurzzeitspektroskopie, Max-Born-Strasse 2A, D-12489 Berlin, Germany

Manfred Faubel

Max-Planck-Institut für Strömungsforschung, Bunsenstrasse 10, D-37073 Göttingen, Germany

Received October 24, 2001

We achieved a continuous, stable, ultrashort pulse hard x-ray point source by focusing 1.8-W, 1-kHz, 50-fs laser pulses onto a novel, 30-μm-diameter, high-velocity, liquid-metal gallium jet. This target geometry avoids most of the debris problems of solid targets and provides nearly 4π illumination. Photon fluxes of 5×10^8 photons/s are generated in a two-component spectrum consisting of a broad continuum from 4 to 14 keV and strong K_α and K_β emission lines at 9.25 and 10.26 keV. This source will find wide use in time-resolved x-ray diffraction studies and other applications.

OCIS codes: 320.5550, 320.7110, 340.7480, 350.5400.

The capability of intense femtosecond lasers to create microplasmas that are strong, short-duration, hard x-ray emitters will introduce powerful new tools to several disciplines of biology, physics, and materials science.[1–4] Impressive demonstrations of the potential of these new kilo-electron-volt light sources for the study of ultrafast solid-state kinetics in semiconductors have already been made, as, for example, in x-ray diffraction studies of coherent acoustic pulse generation and nonthermal melting processes in bulk crystals.[3,4] Ultrafast x-ray diffraction studies have hitherto been possible only with the use of large third-generation synchrotron facilities.[5]

It is well known that direct, nonthermal coupling processes that occur in the interaction of ultrahigh intensity, short-duration laser light with dense plasmas lead to the generation of superthermal electrons. In plasmas generated from solid targets, these electrons then give rise to broadband bremsstrahlung emission and narrow K_α line emission through collisions with, respectively, the hot dense plasma and the cold dense material that surrounds it.[1] In recent years detailed experimental studies have characterized the dependence of this emission over a range of laser and plasma parameters for several different target materials.[6,7] Up to this time most of these studies have been performed in the single-shot or low-repetition-rate (~10-Hz) regime with large multistage femtosecond or subpicosecond laser facilities, as these are the only facilities capable of generating the very high intensities ($\sim 10^{17}$ W/cm^2) required for this interaction regime.[8] In general, simple solid targets or pulsed dense gas jet or cluster targets were used, since the effects of target debris are relatively small in this regime.

For ultrashort x-ray sources to be more widely used, they must become compact and exhibit high average power. Moreover they must operate in a continuous regime with minimal laser adjustment and target replenishment. Developments in both laser and target technology are making this a reality. In the past few years there have been rapid improvements in high-power femtosecond Ti:sapphire laser systems that function at a kilohertz repetition rate, some capable of peak intensities of $\sim 10^{18}$ W/cm^2.[2,9–12]

The plasmas created by high-repetition-rate lasers need target configurations that are continuous in operation, to present each laser pulse with a virgin target surface that remains precisely aligned within the short Rayleigh range of the high numerical aperture focusing optics employed (usually a few micrometers). Targets based on rotating disks, or drum targets, or on reeled tapes or wires have target surfaces many times greater in spatial extent than the focused spot size. This limits the solid angle of the useful x-ray emission from the plasma and, more seriously, leads to the generation of copious amounts of deleterious target debris.[13] The severity of the latter has led to the development of microscopic (10–80 μm) liquid jet or droplet targets that can bring the mass of the target down to that of the number of required radiating atoms.[14] These targets provide long-term, debris-free operation, with almost 4π illumination. However, so far they have been limited to only a few liquids (water,[15] fluorocarbons,[16] copper nitrate solution,[17] ethylene glycol[17]) or gases [N_2,[16,18] Ar,[18] Xe (Ref. 19)]. This is a drawback for hard x-ray generation at high laser intensities where high-Z materials have higher conversion efficiency.

Here we report the use of a liquid-metal jet as a target for a laser plasma. By incorporating the jet with a high-repetition-rate kilohertz high-intensity femtosecond laser, we demonstrate for the first time to our knowledge an efficient, low debris, continuous kilo-electron-volt subpicosecond point x-ray source.[20] As functional targets for high-repetition-rate laser plasmas, liquid jets must provide stable hydrodynamic flow for lengths sufficient to locate the laser focus region far enough from the jet nozzle (i.e., several millimeters) to prevent the latter from adverse plasma effects. The liquid jet decays into a stream of droplets at a distance L from the nozzle exit. For laminar flow conditions the jet decay into droplets occurs at a fixed time interval T, which is a function of the liquid properties listed in Table 1 and of jet diameter d. The actual laminar jet length thus increases with the jet flow velocity v to

0146-9592/02/100866-03$15.00/0

give $L \sim 6.0\ \mathrm{v}\ (\rho d^3/\sigma)^{1/2}$ in the limiting case of inviscid fluids[21] [d is the jet diameter (m), ρ is the liquid density (kg/m^3), σ is the surface tension (mN m^{-1})]. For the 30-μm Ga jet the decay time is $T \sim 0.092$ ms. Or, for a jet with a typical velocity of $v = 30$ ms^{-1} (corresponding to a backpressure of 30 bars), the laminar flow decay occurs 2.8 mm from the nozzle exit. So the decay time of the jet defines the trade-off between maximum laminar jet length (high backpressure) for optimal focusing and low material consumption.

Candidate metal target materials that realistically could be used as a thin liquid jet are those having low melting points and physical characteristics that permit stable jet lengths. Table 1 lists some of these metals, illustrating the availability of a wide range of K_α x-ray emission wavelengths. For use as a laser plasma x-ray target, the liquid metal must also have a flow velocity high enough to ensure that the jet is replenished and restored after each laser pulse. This can easily be achieved with typical flow velocities of 10 to 100 m/s, which will allow repetition rates >100 kHz. In addition the jet's small lateral size, with diameters as small as 10 μm, allows for near-perfect matching to the spatial extension of the laser focus. The narrow spatial confinement of the radiation source provided by this geometry could be favorable for the generation of short x-ray bursts in the 100-fs time range.

The experiments reported here focus on laser plasmas produced from stable Ga jets. For these experiments we used a jet diameter $d \sim 30$ μm. The backpressure was 30–40 bars, which is consistent with jet velocities of >30 ms^{-1} and stable jet lengths of ~3 mm. Experimentally, we determined stable jet lengths of this order with a simple He–Ne laser scattering diagnostic. The liquid Ga jet was located vertically within a vacuum chamber at the focus of an $f = 7$-cm lens (Fig. 1). This focused the output of a high-power, 1-kHz repetition-rate, Ti:sapphire laser system onto the Ga jet to a spot diameter of ~10 μm at ~2 mm from the nozzle. A Ga collector was located below the liquid jet, allowing for continual retrieval and reuse of the target material. The kilohertz femtosecond laser consisted of a cavity-dumped mode-locked Ti:sapphire oscillator, a regenerative amplifier, and a double-pass booster amplifier providing compressed 50-fs pulses at 780-nm wavelength ($\Delta\lambda \sim 25$ nm) with a maximum average power of 1.8 W. A pulse shaper was inserted in front of the stretcher to reduce the phase aberrations created by the stretcher and the optical components. This enabled precise high-intensity target interaction conditions, as well as the use of specially shaped pulses for x-ray generation. The effective contrast ratio of the amplified pulse was ~10^4. The intensity on target was 3×10^{16} W/cm^2.

The spectrum of the x-ray emission that emanated from the plasma was measured with a Si photodiode-based energy-dispersive, x-ray detector (XR-100CR, Amptek, Inc., Bedford, Mass.). It was placed 300 mm from the x-ray source. To avoid pileup effects we positioned a 1.5-mm-diameter pinhole 3 cm from the detector. A 12-μm Al foil placed directly at the detector entrance acted as a cut-off filter for energies below 2.5 keV. The detector output was connected by an amplifier (PX2CR, Amptec, Inc.) to the input of a multichannel amplifier (MCA8000A, Amptek, Inc.). The detector system was energy calibrated by use of a ^{241}Am radionucleide source to a measured energy resolution of 300 eV. An x-ray spectrum from the plasma generated by the Ga liquid jet is shown in Fig. 2. It consists of a broad continuum and two narrow features of 9.2 and 10.3 keV. These two peaks correspond to the characteristic K_α and K_β lines of Ga. The K_α feature has two components, at 9.22 and 9.25 keV, corresponding to the $K_{\alpha 1}$ and $K_{\alpha 2}$ lines, respectively. The broad continuum is predominantly free–free collisional (bremsstrahlung) emission from the plasma; the falloff at the low energy end of the spectrum is due to the transmission characteristics of the Al foil ($T = 0.3$ at 4 keV). The characteristic K_α and K_β lines originate from the collision of the high-energy electrons with cold target material as they propagate forward through the jet, or from those electrons that stream outward from the plasma interaction, toward the laser, are captured by the Coulomb field they create, and stream back into cold jet material in the vicinity of the plasma. The energy dispersive detector also gives an estimate of the absolute photon yield from the source, which was measured to be ~4×10^4 (photons/sr)/pulse. On the assumption of isotropic emission into 4π sr, this would indicate a total emission power of x rays above the Al edge at 2.5 keV to ~5×10^8 photons/s. The K_α line feature was measured to be ~1.5×10^8 photons/s, with intensity fluctuations of the order of 20%. We emphasize that the x-ray flux averaged over 200 s has a constant value to within ±10% for the full experimental run of 1.5 h.

Table 1. Characteristics of Liquid-Metal Jet Laser Plasma Targets[a]

Material	Tm (deg C)	T (deg C)	ρ (kg/m^3)	σ (mN/m)	η (mPa s)	Z	K_α (keV)
Ga	29.8	37	6095	704	1.6	31	9.25
Se	221	250	4818	105	1.2	34	11.22
Rb	39	67	1463	91	0.5	37	13.39
In	156	250	7310	559	1.35	49	24.21
Cs	28	29	1850	73	1.2	55	30.97
Hg	−38.9	25	13594	484	1.52	80	70.82
Water	0	25	997	72	0.89	1.8	0.52

[a]Tm, melting point.

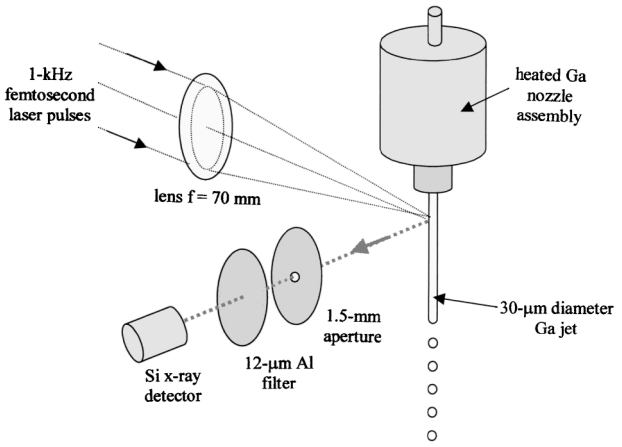

Fig. 1. Experimental arrangement of the liquid-Ga jet laser plasma source.

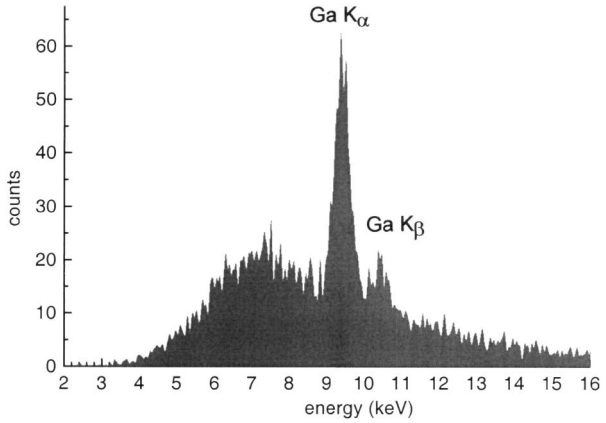

Fig. 2. Spectral emission of femtosecond laser plasma from a Ga jet target.

Most probably the conversion efficiency can be improved by optimization of the laser pulse and irradiation conditions and with the availability of higher-powered lasers. Moreover other target materials will provide a broad spectral range of x-ray emission, either from the plasma continuum emission or from the characteristic K_α and K_β emission lines illustrated in Table 1. During 1.5-h operation time the transmission through the focusing optic did not drop measurably, which points to low-level debris.

The advantages of high-repetition-rate continuous operation of this source, with its relatively benign illumination environment, effectively nearly 4π in extent, without the need for target replenishment, should satisfy many of the requirements of a high-power femtosecond laser hard x-ray source. It should find wide applications in x-ray diffraction studies of solid-state and biological materials and other time-resolved studies, such as x-ray radiography and x-ray fluorescence spectroscopy. Anticipated increases in laser power and intensity capabilities will allow extension of this source to higher x-ray fluxes and higher x-ray energies.

The authors acknowledge useful discussions with J.-C. Kieffer, C. Rose-Petruck, and C. W. Siders on short-pulse high-intensity x-ray generation. This research was supported by the Bundesministerium für Bildung und Forschung, Förderkennzeichen 13 N7923. T. Elsaesser's e-mail address is elsasser@mbi-berlin.de.

*Also with the School of Optics and Center for Research and Education in Optics and Lasers, University of Central Florida, 4000 Central Florida Boulevard, Orlando, Florida 32816-2700.

References

1. J. D. Kmetec, C. L. Gordon III, J. J. Macklin, B. E. Lemoff, G. S. Brown, and S. E. Harris, Phys. Rev. Lett. **68,** 1527 (1992).
2. J. C. Kieffer, M. Chaker, J. P. Matte, H. Pepin, C. Y. Cote, Y. Beaudoin, T. W. Johnston, C. Y. Chien, S. Coe, G. Mourou, and O. Peyrusse, Phys. Fluids B **5,** 2676 (1993).
3. For a review see A. Rousse, C. Rischel, and J. C. Gauthier, Rev. Mod. Phys. **73,** 17 (2001).
4. D. von der Linde *et al.,* Laser Part. Beams **19,** 15 (2001), and references therein.
5. V. Srajer, Tsu-yi Teng, T. Ursby, C. Pradervand, Z. Ren, S.-I. Adachi, W. Schildkamp, D. Bourgeois, M. Wulff, and K. Moffat, Science **274,** 1726 (1996).
6. Ch. Reich, P. Gibbon, I. Uschmann, and E. Förster, Phys. Rev. Lett. **84,** 4846 (2000).
7. D. Perry, J. A. Sefcik, T. Cowan, S. Hatchett, A. Hunt, M. Moran, D. Pennington, R. Snavely, and S. C. Wilks, Rev. Sci. Instrum. **70,** 265 (1999).
8. M. D. Perry and G. Mourou, Science **264,** 917 (1994).
9. J. Squier, G. Korn, G. Mourou, G. Vaillancourt, and M. Bouvier, Opt. Lett. **18,** 625 (1993).
10. V. Bagnoud and F. Salin, Appl. Phys. B **70,** S165 (2000).
11. S. Sartania, Z. Cheng, M. Lenzner, G. Tempea, Ch. Spielmann, F. Krausz, and K. Ferencz, Opt. Lett. **22,** 1562 (1997).
12. O. Albert, H. Wang, D. Liu, Z. Chang, and G. Mourou, Opt. Lett. **25,** 1125 (2000).
13. M. Richardson, W. T. Silfvast, H. A. Bender, A. Hanzo, V. Yanovsky, F. Jin, and J. Thorpe, Appl. Opt. **32,** 6901 (1993).
14. F. Jin, K. Gabel, M. Richardson, M. Kado, A. F. Vassiliev, and D. Salzmann, Proc. SPIE **2015,** 151 (1993).
15. M. Richardson, D. Torres, C. DePriest, F. Jin, and G. Shimkaveg, Opt. Commun. **145,** 109 (1998).
16. M. Berglund, L. Rymell, H. M. Hertz, and T. Wilhein, Rev. Sci. Instrum. **69,** 2361 (1998).
17. R. J. Tompkins, I. P. Mercer, M. Fettweis, C. J. Barnett, D. R. Klug, Lord G. Porter, I. Clark, P. Matousek, A. W. Parker, and M. Towrie, Rev. Sci. Instrum. **69,** 3113 (1998).
18. M. Wieland, T. Wilhein, M. Faubel, Ch. Ellert, M. Schmidt, and O. Sublemoutier, Appl. Phys. B **72,** 591 (2001).
19. B. A. M. Hansson, L. Rymell, M. Berglund, and H. M. Hertz, Microelectron Eng. **53,** 667 (2000).
20. G. Korn, A. Thoss, M. Faubel, H. Stiel, U. Voigt, M. Richardson, and T. Elsaesser, in *Conference on Lasers and Electro-Optics (CLEO)*, Vol. 56 of OSA Trends in Optics and Photonics Series (Optical Society of America, Washington, D.C., 2001), paper CTuC4.
21. M. Faubel, in *Photoionization and Photodetachment*, C. Y. Ng, ed. (World Scientific, Singapore, 2000), p. 634.